Dimensional stability of Electric Arc Furnace slag in civil engineering applications

Amaia Santamaria [(1)], Flora Faleschini [(2,3)], Giovanni Giacomello [(2)], Katya Brunelli [(3,2)], José-Tomás San José [(1)], Carlo Pellegrino [(2)], Marco Pasetto [(2)]

[(1)] *Universidad del Pais Vasco - Euskal Herriko Unibertsitatea, Campus Bizkaia, Department of Materials Science, Bilbao, Spain.*

[(2)] *Department of Civil, Environmental and Architectural Engineering, University of Padova, Padova, Italy.*

[(3)] *Department of Industrial Engineering, University of Padova, Padova, Italy.*

Highlights

- Swelling of EAF slag due to free CaO hydroxilation is experimentally investigated.
- EAF slag surface enriches of calcite after weathering.
- Open porosity is reduced after weathering, improving slag properties.
- Limits for maximum allowable slag swelling are provided for some applications.

Abstract

Dimensional stability of manufactured aggregates represents a matter of interest for many applications in civil engineering. Past results evidenced how steel slag might be affected by potential swelling, due to several concurring causes linked to the presence of free lime and periclase in their chemical composition. In this work, a detailed analysis about physical and chemical properties of Electric Arc Furnace slag (EAFS) is developed, using thermogravimetry, scanning electron microscopy, X-ray diffraction and porosity analysis. The efficiency of a commonly used method for slag treatment on reducing its swelling-potential is also experimentally assessed and confirmed, through expansion tests carried out in an experimental apparatus developed specifically for this scope, based on steam diffusion within the test sample. Lastly, a maximum allowable limit for slag swelling is proposed for some applications of interest.

Keywords

EAF slag; constructions; expansion; manufactured aggregates; microstructural analysis; recycling.

1. Introduction

Iron and steelmaking industry is a very important activity for the economies all over the world. However, it consumes a large amount of raw materials and energy, and yields a large amount of waste, among which slags are the most abundant. In Southern Europe, the most common way for manufacturing steel is through the Electric Arc Furnace (EAF) technology; more than 40% of steel produced in Europe in this type of furnace is manufactured in Italy and Spain (Worldsteel association, 2015), and hence huge amount of Electric Arc Furnace Slag (EAFS) should be managed in these countries. Steel slags are formed from added fluxes, iron oxides and impurities of iron and steel scraps originated during melting and oxidizing processes. After separation from melted steel, slags are cooled with different manners (depending on the production technique) and stockpiled.

Nowadays, slag stockpiling is gaining increasing importance because of the large amount of steel waste produced each year. Steel slag re-utilization in civil works is becoming an intensive business, guaranteeing several benefits related to the environmental safeguard in terms of natural resources preservation (avoiding onerous quarrying processes) and waste disposal reduction.

An essential feature towards the sustainability of the planet and a circular economy is promoting the use of waste as raw materials. Currently, construction and civil works industry is one of the largest consumers of waste materials. Akinmusuru (1991), Geiseler (1996), Motz and Geiseler (2001) and Koros (2003) first proposed the use of steel slag in construction industry. Other than these authors, many researchers developed a significant research in this field (Al-Negheimish et al., 1997; Shelburne and DeGroot, 1998; Bignozzi et al., 2010; Colorado et al., 2016; Faleschini et al., 2014; Manso et al., 2013; Oluwasola et al., 2016; Pasetto and Baldo, 2006; Adegoloye et al., 2016; Skaf et al., 2016). The main uses proposed for the electric arc furnace slag are as aggregates in bituminous (Ameri et al., 2013; Bosela et al., 2009; Fronek, 2012; Fronek et al. 2012; Kavussi and Qazizadeh, 2014; Pasetto and Baldo, 2011; Skaf et al., 2017; Yildirim and Prezzi, 2009) and hydraulic mixes (Anastasiou et al., 2014; Faleschini et al. 2015; Faleschini et al., 2017; Kim et al., 2013; Papayianni and Anastasiou, 2010; Pasetto and Baldo, 2016; Pellegrino and Faleschini, 2013; Sekaran et al., 2015), because of its good characteristics of stiffness, strength and durability.

Due its appearance as gravel (fine-coarse aggregate), laboratory and in-situ research concerning EAFS re-use in road infrastructure demonstrated good results for asphalt and cement bound mixtures production. The main reasons to justify this affordable re-use are principally due to comparable or even enhanced performance in terms of stiffness, rutting potential, fatigue and skid resistance (Pasetto and Baldo, 2012; Pasetto and Baldo, 2014; Oluwasola et al., 2015; Pasetto et al., 2016; Pasetto et al., 2017) than alternative aggregates. Also the mechanical properties (Arribas et al., 2015; Fuente-Alonso et al. 2017; Pellegrino et al., 2013; Santamaría et al., 2016) and durability (Arribas et al., 2014; Manso et al., 2006; Monosi et al., 2016; Morino and Iwatsuki, 1999; Ortega-Lopez et al., 2018) of concrete manufactured with this slag have been demonstrated to be similar, or even better, than concretes made with traditional (natural) aggregates.

According to these results, some constructors have employed EAFS in real construction works (Arribas et al., 2010; García Mochales, 2016). Among the available standards for aggregates used in civil engineering applications, there is not a complete one that regulate EAFS use, but only some guidelines are provided (IHOBE, 1999). The European standard EN 12620 (2002) defines the characteristics of “Aggregates for Concrete” and it classifies this kind of slag as a manufactured aggregate, however it does not account neither for slag potential volumetric expansiveness, nor for the other peculiar slag properties. Slag potential expansiveness is one of the key problems which might hinder slag applicability as a construction material, because it may cause severe damage in construction works, as it is shown in Figure 1.

Figure 1: Effects of slag expansion in some kerbs.

Five main reactions have been found to be responsible for EAFS potential swelling at outdoor temperature (Tomellini, 1999; Arribas et al 2015):

- The evolution of dicalcium silicate β to γ allotropic form. Due to the presence of P_2O_5 and other β-phase stabilizers in the EAFS, this reaction is not frequent.
- The long-term oxidation of metallic iron from iron +2 to iron +3 (not usual in EAFS).
- Hydroxylation of free CaO and subsequent carbonation, in presence of moisture.
- Hydroxylation and carbonation of free MgO.
- Hydration of calcium aluminates, associated to a minor expansion.

The most common expansive reaction is the hydroxylation and carbonation of free lime.

Some authors have previously shown that free lime in steel slags can be found in two different morphologies, determined as “primary” and “secondary” (Geiseler and Schlösser, 1998; Ortega-López et al., 2014; Pellegrino et al., 2013; Waligora et al., 2010). Free lime known as “primary” is the undissolved lime previously described, being a grainy or spongy solid phase suspended in the liquid slag. In non-hydrated slag, it is possible to find free CaO with particle sizes of 4-60 µm.

“Secondary” free lime, also known as precipitate free lime, may be found in the grain boundaries of some iron oxide-based compounds (dicalcium ferrite or R-O phase), and dispersed in calcium silicates. Its size is usually in the range of 4 to 20 µm. This free lime has a slower interaction with the environment than the “primary”, due to its slower diffusion, and normally it is present in lower amount than the primary (Wachsmuth et al., 1981).

Hydroxylation and carbonation of free lime result always in a volume increase. Some authors have studied the swelling of such steel slags due to the presence of this compound (Autelitano and Giuliani, 2015; Brand and Roesler, 2015; Coppola et al., 2010; DePree and Ferry, 2008; Pellegrino et al., 2013; Wang et al., 2015; Yildirim and Prezzi, 2011). Wang (2010) and Wang et al. (2010) have studied this phenomenon, and have proposed a theoretical equation for predicting volume expansion of steel slag. Other researches (Frías et al. 2010; Manso et al., 2006) have highlighted that the swelling of this slag can be easily reduced. The hydroxylation of “primary” free lime is a reaction that usually occurs in few days or weeks, so a weathering period of 90 days after slag crushing was found to be effective to stabilize the slag, in presence of moisture.

At present, in the European Union (EU), there is not a fixed method to predict the volumetric expansion of the EAFS, due to the high number of variables that influence this phenomenon, and even it neither exists a well accepted or agreed value for a maximum allowable slag swelling, to be used in bituminous and/or concrete mixes. Additionally, the diffusion process of free lime is not even well known, and doubts exist about if the hydroxylation process happens in the surface of the slag particles only, or if it occurs inside the particles too. Slag porosity, chemical composition, particles shape are some of the variables that influence steel slag swelling potential. There are still many questions open about the expansion of the EAFS, and this paper aims to try to answer to some of them.

Hence, in this research, a detailed analysis about chemical properties of electric arc furnace slag has been developed, trying to evaluate the influence of its expansive compounds. Several expansion tests, in accordance to the European Standard EN 1744-1:2013 (developed specifically for other kinds of slag), have been carried out in fresh and weathered EAFS, for a better understanding of the phenomenon of volumetric expansion of such material. This test method has been proved to be effective for studying EAFS swelling due mainly to free CaO hydroxylation.

2. EAFS characterization

Black oxidizing EAFS comes due to the addition of fluxes, other oxides as lime and burnt periclase and the oxygen blowing, in the electric arc furnaces during steelmaking; it is separated from the bath of steel due to specific weight difference, being the melted slag floating at the surface. Then, it is cooled from the temperature of about 1300°C to ambient conditions, typically through water spraying, in a relative short time. Alternatively, blocks may be solidified in outdoor conditions, thus implying a longer process. In both cases, and mainly in the latter, a certain amount of free calcium and free magnesium oxides may be entrapped in the slag; these two compounds represent the main potential source of expansive reactions in this material, when moisture is present. Hence, it is expected, in general terms, that slag characteristics in the so-called “fresh state” differ from those after weathering (Tomellini, 1999).

Accordingly, in this work an experimental campaign aimed to characterize an EAF slag is carried out; physical properties, chemical composition, morphology and microstructure are analyzed in the following sections. One kind of slag produced in a steelmaking facility in north Italy has been analyzed at two stages: in the “fresh state”, i.e. at 1-2 days after cooling; and in the “weathered state”, i.e. after 3 months of exposure at atmospheric conditions, processing as an aggregate (sieving, crushing, metallic iron removal, etc.) and one week of daily wetting-drying cycles. In the initial liquid state after pouring, slag is cooled through water-spaying, and this process lasts one day. The cooling method could influence slag physical and chemical characteristics at long term, as some of the same authors of this paper have highlighted in a previous work (Santamaria et al., 2017), even though it is not considered as a variable for this study, being the cooling procedure the same for both the “fresh slag” and the “weathered” one. Concerning weathering time, also this variable is known being an influencing parameter for slag characteristics (Santamaria et al., 2017). However, most of the scientific literature agree identifying a maturation time of 3 months as a suitable weathering period (Manso et al. 2006; Pellegrino and Gaddo, 2009; Pellegrino et al., 2013), and many practitioners have adopted such method in the current practice, both in Italy and Spain. Other criteria can however be identified to establish the condition of “weathered slag”.

Table 1. Oxide composition of the analyzed EAF slag at the fresh state.

Oxides	MgO	Al_2O_3	SiO_2	CaO	Cr_2O_3	MnO	FeO/Fe_2O_3
Amount in %	2.8	10.5	16.3	26.8	2.6	5.6	35.4

The chemical composition of the oxidizing slag is listed in Table 1 and it can be considered as a “typical” EAFS, even though the content of iron oxides might vary significantly among slags produced in different facilities. Indeed, its composition lays within the typical range of EAFS from carbon steel production, as it can be observed comparing oxides content with ones listed in the experimental dataset collected by Pellegrino and Faleschini (2016). The most abundant oxides are FeO/Fe_2O_3, CaO, SiO_2 and Al_2O_3. A notable density can be also expected, at least as a rough estimation, because the after-blowing iron-manganese-chromium oxides density exceeds 5000 kg/m^3, while the rest of oxides combine in form of compounds with a density lower than 3000 kg/m^3.

The slag appears as a stony material, with high density and low porosity, with few particles characterized by higher porosity at macroscopic sight. Its color, in the fresh state, varies from black to dark-grey; conversely, it becomes light grey after ageing. Figure 2 shows the color change with time of a fresh slag particle, respectively 2 and 9 days after slag cooling. Locally, white powder appears at the surface.

Figure 2. Slag appearance: 2 and 9 days after cooling.

Concerning its specific weight, slag can be considered as a heavy-weight artificial aggregate: indeed, it is characterized by an apparent density of almost 4000 kg/m^3, which value slightly changes depending on the slag age and particles dimension. However, it should be recalled that fluctuations in iron oxides content and vacuolar porosity value might lead to significant variations in the specific weight of EAFS, i.e. from 3000 kg/m^3 to 4500 kg/m^3. In this case, fresh slag, which has a mixed grading as it is unprocessed, has an apparent density of about 3750 kg/m^3; whereas, the values of the apparent density for the weathered slag are 3970 kg/m^3, 3950 kg/m^3, 3900 kg/m^3 and 3800 kg/m^3, respectively for the 4-8 mm, 8-12 mm, 12-16 mm and 0-4 mm grading fractions. The water absorption WA% is higher in the fine fraction and at the fresh state, than in the other cases. Indeed, WA% values range between 1 and 1.5% at the fresh state and for the 0-4mm fraction, in the weathered condition; values decrease less than 1% for the weathered coarse fraction. Therefore, these values are close to those of natural aggregates typically employed in civil engineering applications (Mehta and Monteiro, 2013).

Another physical property analyzed in this work is the porosity. From an extensive review of literature, it emerges that there is a significant scatter between the specific weight of slags used among many research works. This difference may be due to a different structure and porosity of the slag, other than to its composition and content of heavy-weight elements. Hence, Mercury Intrusion Porosimetry (MIP) tests are carried out to evaluate slag porosity and density through a more accurate method, than the macroscopic one based on pycnometer test. Tests are carried out with a Thermo Scientific Pascal Mercury porosimeter, on three samples of fresh slag: two are taken from the superficial layer of the stockpile (samples 1 and 2), whereas one is taken from an inner layer (sample 3). Three further samples of weathered slag particles are analyzed, which at macroscopic sight seem structurally similar (samples 4-6).

Pore volume distribution is obtained analyzing Figure 3(a,b), where the incremental pore volume (in percentage) is plotted against pore size diameter. Figure 3a refers to fresh slag particles; it is worth to note that samples 1 and 2 display a similar internal structure, which is made mainly by low size pores. The measured porosity values of these two samples is 1.76% and 2.23% respectively, whereas the measured bulk density is 3890 kg/m^3 and 3980 kg/m^3. Conversely, sample 3 has a relevant number of pores within both the micrometer and nanometer scales, being thus more porous than the previous (porosity of 7.78%). The measured bulk density is 3850 kg/m^3, which agrees with the higher porosity value obtained.

Figure 3b shows instead the incremental pore volume curves of weathered slag: also in this case, two samples display similar structure, whereas the third has more pores with low diameter size (within the nanometer scale). Indeed, 30% of the porosity has less than 10nm in sample 6. It is worth to note that in this case the precision of the instrument was less detailed than in the previous analyses, due to laboratory constraint, and hence it is not possible to better identify how exactly the curve tail is constituted. The measured porosity of samples 4, 5 and 6 is 2.69%, 0.96% and 0.49%, respectively. These values are significantly less than the ones observed for the fresh slag, and this may be related to the advanced stage of slag ageing and stabilization after the maturation protocol;

during ageing, pores can be partially filled by new expansive compounds. Concerning the measured bulk density of the samples, the values obtained with MIP analysis are consistent with the porosity results, and are 3770 kg/m^3, 4280 kg/m^3 and 4260 kg/m^3, in average higher than the ones obtained for the fresh slag. This result also confirms the macroscopic test made with the pycnometer, which provided higher density of the weathered than the fresh slag.

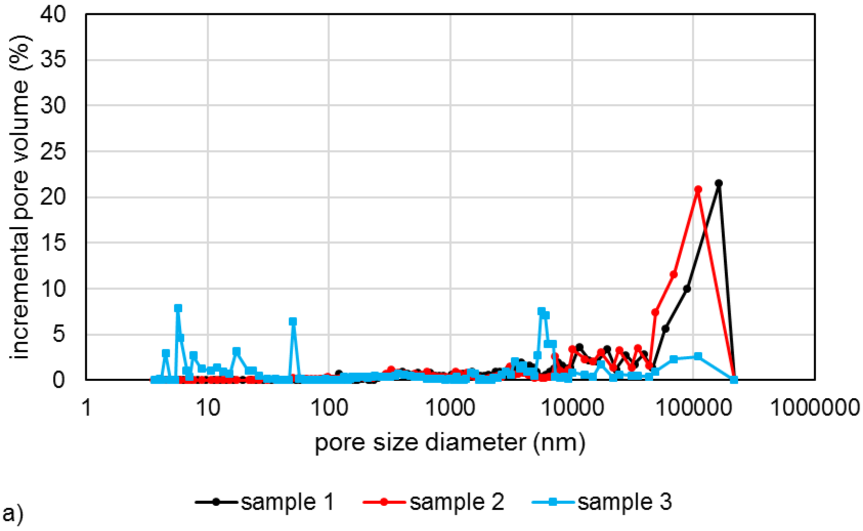

a)

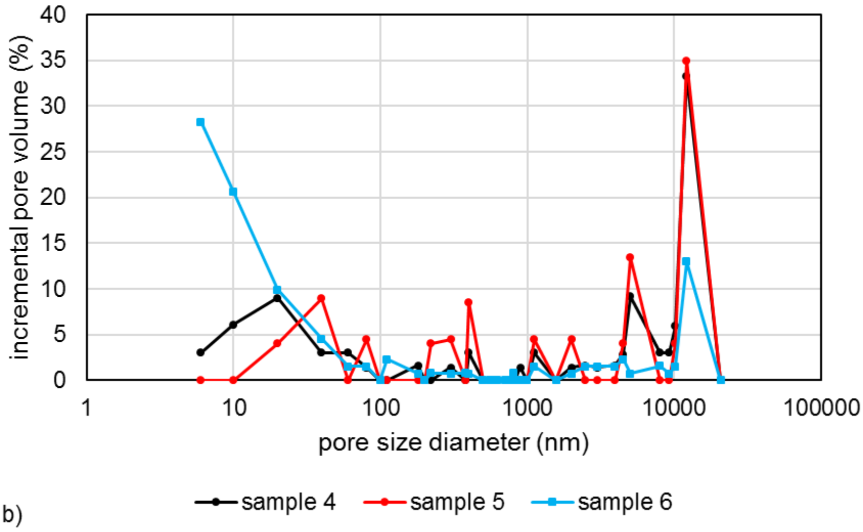

b)

Figure 3. Incremental (percentage) pore volume curves of: a) fresh slag particles; b) weathered slag.

Additional information about the interconnection of the pores can be obtained looking at Figure 3(a,b), which show the cumulative pore volume curves. Concerning the overall amount of mercury, it is significant that the intrusion volume in sample 3 is 0.022 mL/g, about one order of magnitude greater than in other two samples (sample 1: 0.0045 mL/g; sample 2: 0.0056 mL/g). This result indicates that samples 1 and 2 have a close structure, which means that these slag particles are almost impermeable. Conversely, the third sample shows an interconnected structure, more porous, with a structure which can be compared to that of a cement-based material. This may be explained by the fact that this sample, extracted from an inner layer of the fresh stockpile, and already cooled, might be subject to high thermal cycles. Indeed, when the first layer of slag is cooling, which occurs in a relative short time as the thickness is still small, further liquid slag discharges may be carried out, thus implying severe thermal loads for the bottom material. This thermal stress induces the formation of microcracks in the slag particles, which per se increases particles porosity, because the internal porosity due to the presence of occluded gases in the slag becomes accessible. Another possible explanation for this different porosity is that allotropic changes of some slag components are also probable. Changes in dicalcium silicate from β to γ,

decomposition of tricalcium to dicalcium silicate, evolution of iron +2 to iron +3 (wustite-magnetite-hematite system) are reactions that occur between 150°C and 1300°C, which is the same temperature range of slag cooling process. Looking instead at Figure 3b, it can be noted that the cumulative pore distributions are similar for the weathered slag, and they reflect the different porosity values obtained. Also in absolute terms, the overall amount of mercury intruded is within the same range, and it is similar to the amount observed also for samples 1 and 2.
Table 2 summarizes some of the main physical properties of the slag: apparent density and water evaluated with the pycnometer method, and bulk density and porosity measured with MIP test.

Table 2. Physical properties of EAFS.

	Fraction	Apparent Density (kg/m^3)	Water Absorption (%)	Bulk density (kg/m^3)	Porosity (%)
Fresh slag	Mixed	3750	1 – 1.5	3850	1.76-7.78
Weathered slag	0-4 mm	3800	1 – 1.5	3940	2
	4-8 mm	3970	< 1	4270	0.49-2.69
	8-12 mm	3950			
	12-16 mm	3900			

2.1 SEM-EDS analysis

Slag morphology is analyzed through an experimental campaigned carried out with Scanning Electron Microscopy (SEM), equipped with Energy Dispersive X-Ray Spectroscopy (EDS). Images are taken in the backscattered-electron (BSE) mode, on slag surface, before and after particles weathering, with varying resolutions.

Figure 4 shows the surface of a fresh EAFS sample: from an EDS analysis carried out on an extended area of the sample shown in Figure 4a, about 35% by mass is constituted of Fe oxides, whereas Ca and Si oxides represent about 25% and 15%, respectively. Al, Mn, Mg and Cr oxides are also found on the surface of the sample. Looking in detail at Figure 4b, it is worth to note that a complex structure is present, which is mainly characterized by lighter zones (points 1), rich in Fe (with a lower amount of Mg, Mn and Ca), and by darker zones (points 2) that contain principally Ca and Si, and sometimes Al. The former suggests the presence of a solid solution of (Fe, Ca, Mn, Mg)O, structurally close to wüstite, in agreement with the results obtained by XRD analysis. The latter, i.e. darker zones, can be instead attributed to larnite and gehlenite phases, in accordance with X-ray diffraction (XRD) analysis, which results are shown in the next section. The presence of free CaO and MgO was not detected.

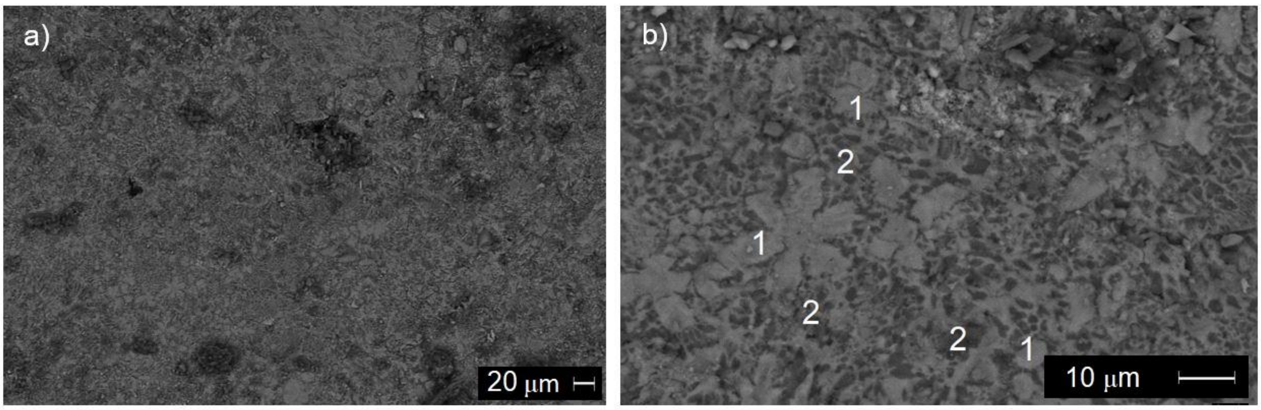

Figure 4. BSE-SEM photo of fresh slag particles: a) low magnification; b) high magnification.

Figure 5 shows instead the surface of a EAFS sample subject to standard weathering, as performed in the treatment plant, where slag is managed. In this case, the morphology appears irregular and with the presence of fragmented and isolated particles, in comparison with fresh sample surface. A superficial layer, very thin, of light-grey color covers the particles: according to an extended EDS analysis, it is possible to detect an increased amount of Ca oxide, if compared to the previous case. Indeed, the composition (by mass) is made mainly by Ca, Fe and Si oxides, being respectively about 45%, 28% and 9%. It is worth to note that the weathered slag surface is enriched in Ca oxides, which content is significantly increased if compared to the case of fresh particles. The darker particles, the most abundant on the surface, (points 1) resulted to be constituted by Ca, O and C, suggesting the presence of $CaCO_3$. The grey zone (point 2) was constituted by Ca, Si and Al oxides, whereas the white particles (points 3) were rich in Fe oxides.
Such results can be compared also with the ones obtained in weathered slag cross-sections, as carried out in Faleschini et al. (2016). In that case, slag particles were cut in half and analyzed. SEM-BSE image of such samples revealed the same constituents found on the fresh slag surface.

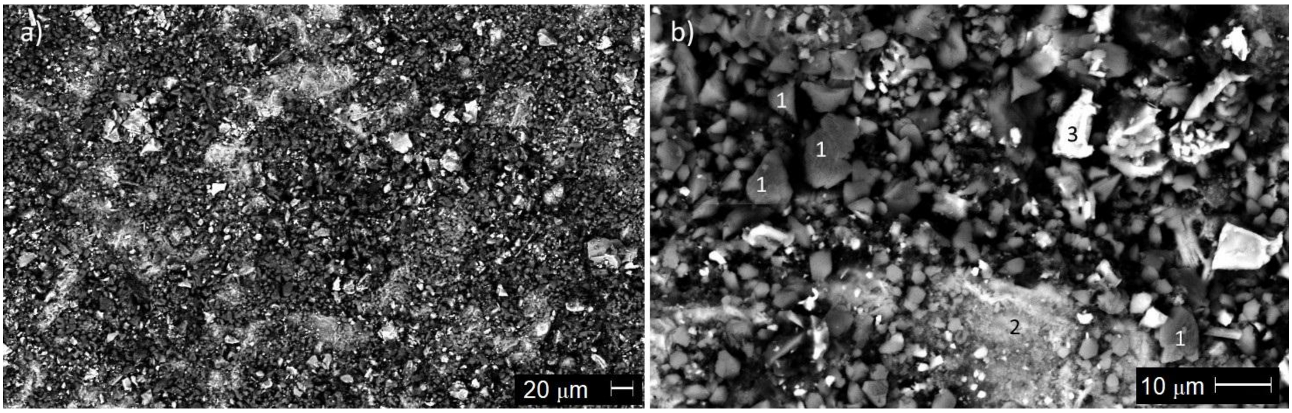

Figure 5. BSE-SEM photo of weathered slag particles: a) low magnification; b) high magnification.

2.2 XRD Analysis

Slag mineralogy is investigated through X-Ray Diffraction (XRD) analysis, obtained for samples of fresh and weathered coarse slag particles. Particularly, XRD analyses are carried out both on the surface of the slag (particles with a planar surface were chosen), and on pulverized samples. Tests are carried out using a Siemens D500 diffractometer, with a stepped and continuous scanning device, and CuKα radiation (λ=1.5405 Å); operating conditions of 40 kV and 30 mA are used.
Concerning the mineralogic composition of the slag surface, the main phases obtained in the fresh slag are wüstite (FeO), magnetite (Fe_3O_4), larnite (Ca_2SiO_4) and gehlenite ($Ca_2Al_2SiO_7$), Figure 6a. Conversely, in the weathered slag, the main peaks are related to the presence of calcite, wüstite, magnetite, larnite and gehlenite (Figure 6b). This result confirms the evidence obtained with the SEM-EDS analysis, through which it was possible to observe an enrichment of Ca oxides content on slag surface, directly correlated to the presence of calcite, which gives the light-grey color to the weathered slag.

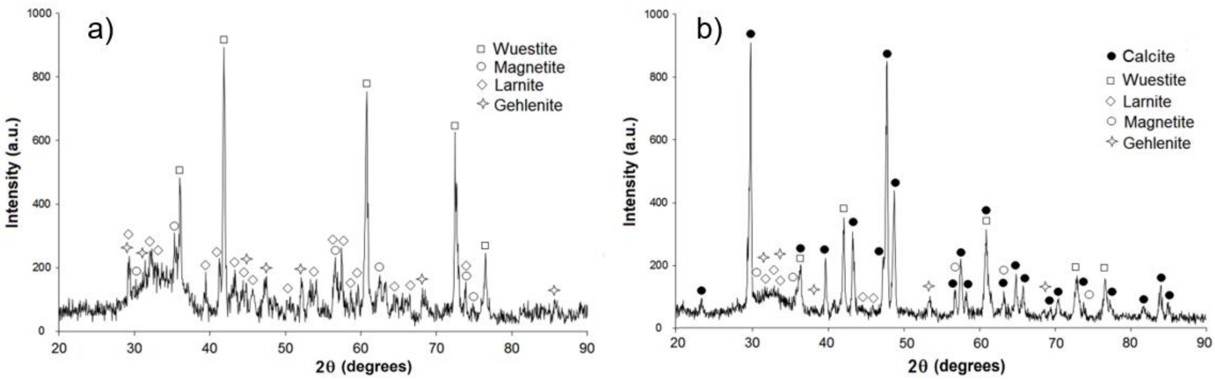

Figure 6. XRD pattern obtained for the surface of: a) fresh slag and b) weathered slag particles.

The XRD patterns obtained with the pulverized slag samples are shown in Figure 7. In this case, the powder was obtained both with the fresh slag and the weathered slag samples. Additionally, the powder resulting from the fresh slag sample was subject to a further weathering process lasting for 7 days.

As it can be observed, the patterns of the powder coming from the fresh slag (Figure 7a) and weathered slag (Figure 7b) are very similar, and the main phases detected are wüstite, magnetite, larnite and gehlenite. These phases are the same found on the surface of the fresh slag samples. Instead, the weathered powder of the fresh sample (Figure 7c) was characterized by the presence of calcite. Therefore, it can be concluded that calcite presence seems mostly related to a superficial enrichment.

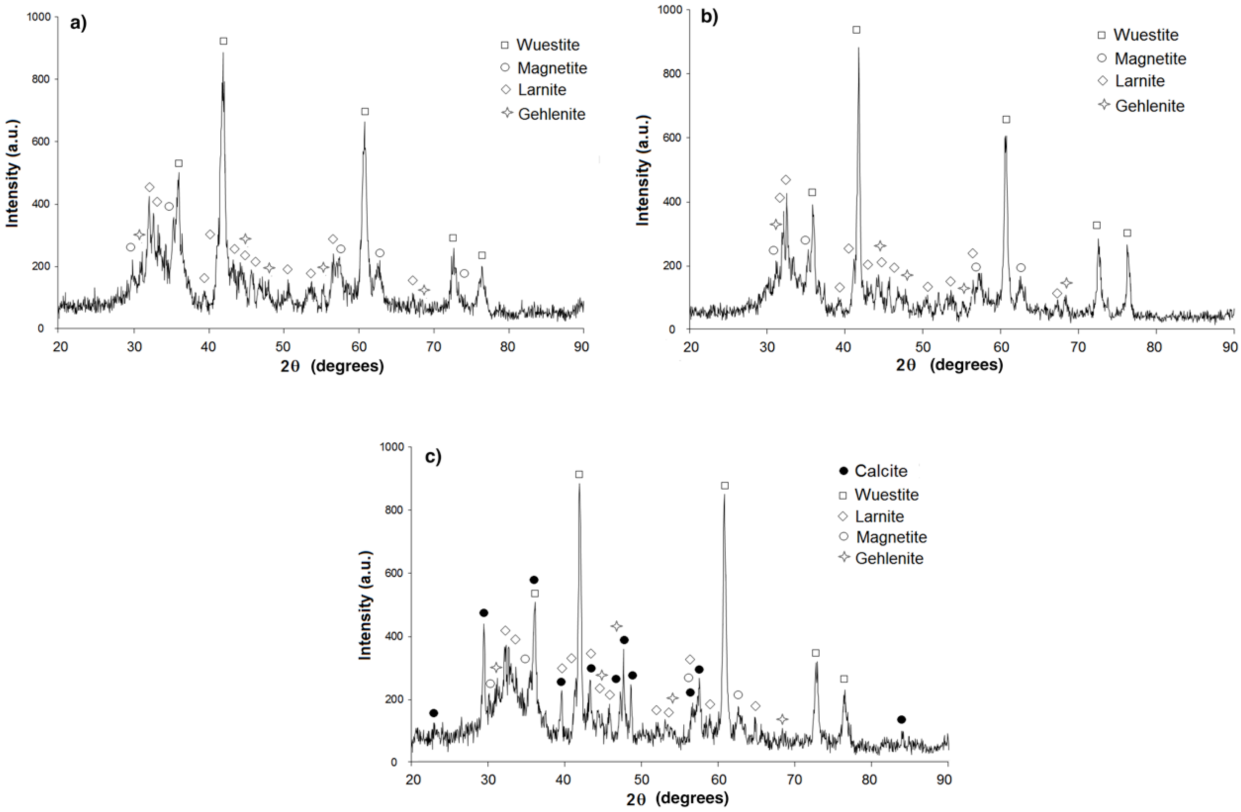

Figure 7. XRD pattern obtained for pulverized samples of: a) fresh slag and b) weathered slag; c) powder of fresh slag weathered for 7 days.

2.3 TGA-DTA analysis

Thermogravimetric Analysis (TGA) and Differential Thermal Analysis (DTA) techniques were used to further characterize both fresh and weathered EAFS. The first allows studying the variation of chemical and physical changes of a material, depending on the temperature, whereas DTA results provide information regarding the physical phenomena occurring in a temperature range. A Nietzsch STA 429 model was used, with a heating rate of about 9°/min, up to 1200°C.

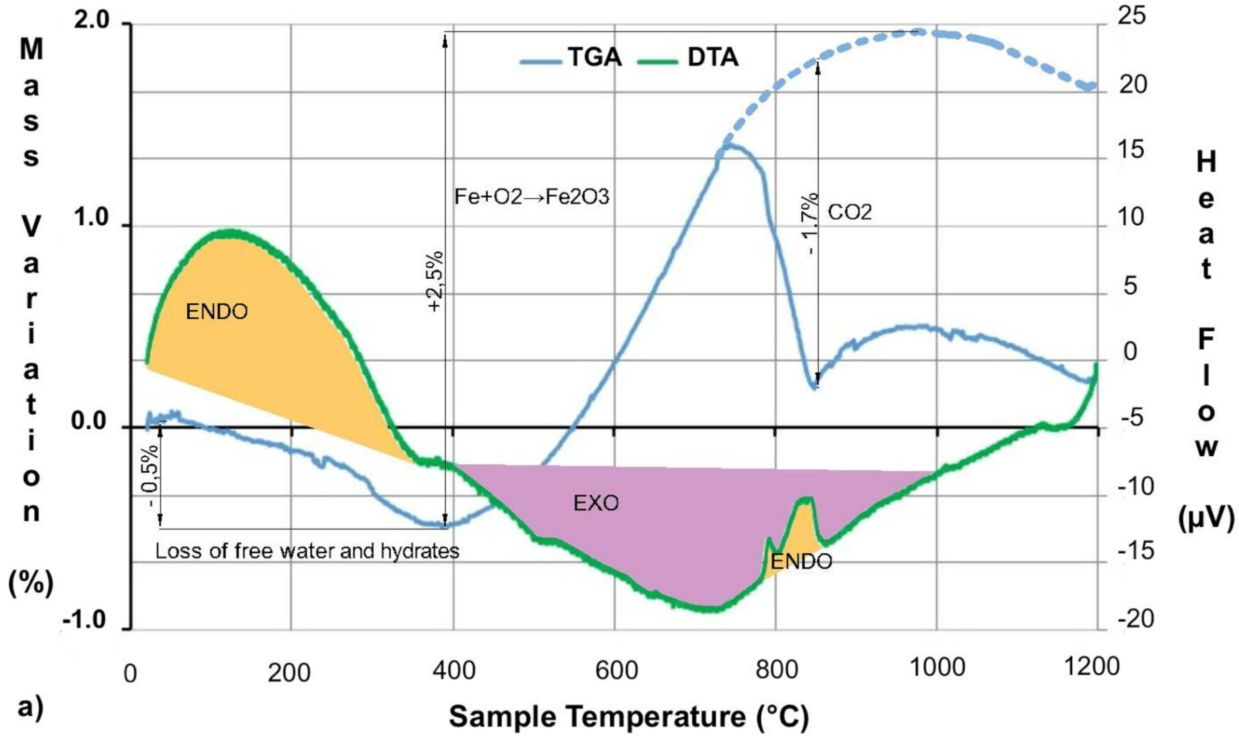

a)

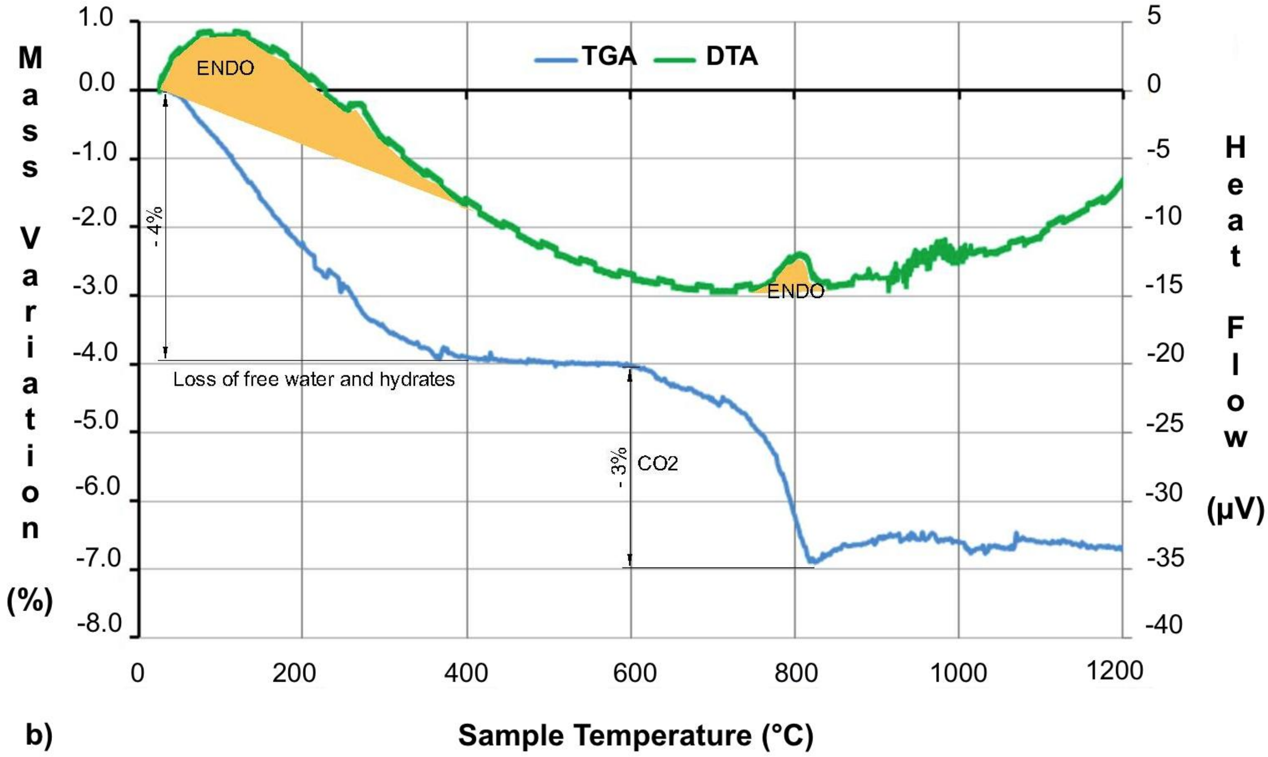

b)

Figure 8. TGA and DTA curves obtained on: a) fresh slag and b) weathered slag.

Figure 8 shows the result of this analysis on fresh slag sample (Figure 8a) and weathered sample (Figure 8b). In the case of fresh slag, loss of free water can be seen before 120ºC, and water loss of other hydrated minerals (low proportions of amorphous calcium aluminates and silicates easily hydratable) until 380ºC. The mass loss is 0.5% due to endothermic reactions, as showed by the enthalpy curve. From 400ºC to 1000ºC a mass gain can be appreciated, that can be attributed to the oxidation of metallic iron, always present in the oxidizing slag in proportions over 5%. The mass gain is in the order of 2.5%, corresponding to the stoichiometry of the oxidation from Fe^0 to Fe^{+3}. In the enthalpy curve an exothermic zone is observed. Together with the above mentioned reactions, dehydroxilation of calcium hydroxide and decarbonation of calcium carbonate can be expected. In Figure 8a, a mass loss or enthalpy variation of calcium hydroxide at 450ºC cannot be observed, but within the region of 800ºC an enthalpy peak and the mass loss of calcium carbonate decomposition can be easily identified. The mass loss is about 1.7%, corresponding to a calcite content of 3.9%, due to a free lime content of 2.2%. Finally, between 1000º and 1200ºC, a slight loss of mass and an endothermic process appear, corresponding to the loss of an unknown substance of low interest in this study.
Concerning the weathered slag, shown in Figure 8b, some of the above described phenomena are again present. Over 120ºC the moisture water is removed (amount about 1%), and from 12º to 400ºC some hydrated compounds loose water in an amount of 3%, clearly higher than in the fresh slag. These phenomena correspond to an endothermic region in the enthalpy curve. From 400ºC, the oxidation of metallic iron is not observed, and in the region of 400º-500ºC no dehydroxilation is displayed. In the interval ranging between 600º and 800ºC, decarbonation of calcite is observed, with an endothermic peak associated to an amount of 3% of carbon dioxide, corresponding to a content of 6.8% of calcite; this content is own to the slag surface, as it was shown in Figure 7b. Finally, a slight mass gain is visible in the interval 820º-950ºC, and a mass loss in 950º-1200ºC, both having low importance in this study.

3. EAFS expansion: experimental methods

Expansion tests are performed with an apparatus realized by the researchers of the University of Padova. Following the standard EN 1744-1:2013 “Tests for chemical properties of aggregates, Part 1: Chemical analysis”, the apparatus is composed by: a steam generator (the water is heated up to boiling point with a heating coil, producing the steam), an isolated pipe (to transport the steam from the generator to the sample), a chamber, a perforated base, a mold and the sample.

The chamber is a steel hollow cylinder, with an internal diameter of about 150 mm and a height of about 120 mm, closed and welded at the extremities by two steel plate square-shaped. The plate on the top is drilled in the center with a diameter equal to that of the cylinder. The perforated base is a steel square-shaped plate and, similarly to the chamber, the base has four holes. In addition, the perforated base has 49 holes (3 mm diameter), as indicated by the standard. The mold is realized with a hollow steel cylinder (diameter 150 mm and height 120 mm) too, that contains the slag sample. Chamber, perforated base and mold are mounted together with four bolts/nuts, one for each vertex. According to EN 1744-1, a fabric mat (filter paper) is placed between the perforated base and the sample; another fabric mat, a glass beads (5 mm diameter) layer, a perforated plate (30 % open area), a surcharge support (to allow the steam passage) and a surcharge are placed on the top of the slag sample. The overall load on the slag sample is about 7.5 kg. All the parts have been insulated with foam-rubber to prevent heat dispersion. On the top of surcharge, a displacement indicator is placed (see Figure 9a).

The steam flow produced by the generator machine arrives in the chamber and passes through the sample. The amount of slag particles is about 2.32 kg for each test sample, using an analogy in terms of vapor flux passing through a sample with standard dimensions. Time of testing is fixed at 24 hours, even though after 8 hours no expansion increase is detected anymore. During the test, steam interacts with free calcium oxide particles and high temperatures favor the expansion acceleration, making it possible to measure the expansion through the indicator placed on the top of the apparatus. The steam interacts with the free magnesium oxide particles too, but their expansion is much lengthy over time.

Test procedure follows the standard EN 1744-1. Slags are sampled, dried, sieved and then are combined together to realize the test sample. EAFS size ranges from 0 mm to 22 mm (Figure 9b), and the overall grading follows the Fuller grading curve. Subsequently, slags are compacted in the mold, which is placed and connected to the chamber as previously described. Displacements measurement starts when steam vapor is visible through the sample. As required by standard, measurements were performed each 15 minutes during the first 4 hours, then each 30 minutes. Expansion results were expressed in terms of percentage variation over the original sample volume.

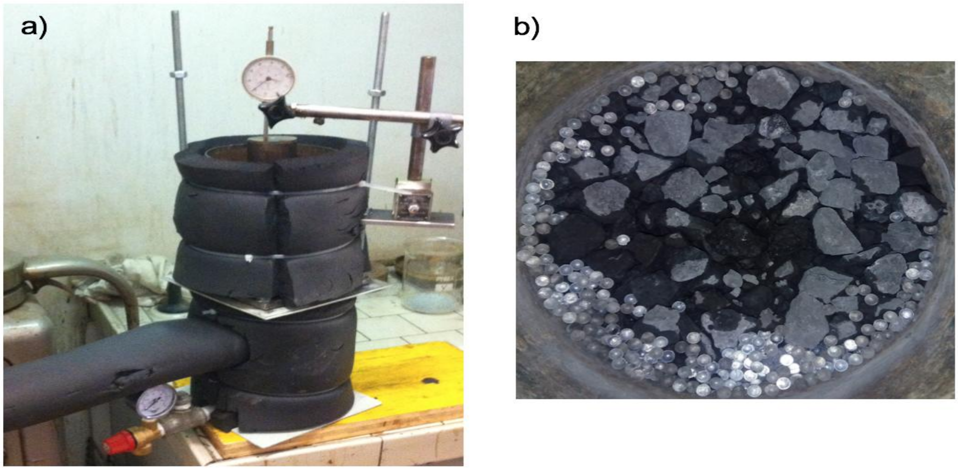

Figure 9. a) Chamber and molds of the expansion apparatus; b) slag particles sample inside the mold.

4. Results and discussion

Results obtained in triplicate of fresh slag displayed global values of swelling ranging between 1.54% and 2.06% (see Figure 10a), evidencing that after one hour of test, the corresponding swelling is about 2/3 of the final value. This circumstance demonstrates the efficiency of the test to perform the hydration of expansive slag compounds. The strongly cloistered (Ortega-Lopez et al., 2014; Herrero et al., 2016) free CaO takes several hours to reach total hydration, as well as in the case of magnesium oxide.
Results of the tests carried out in triplicate of weathered slag showed lower expansion values than in the former case, being 0.72%, 0.58% and 0.33% (Figure 10b). Some of them are higher than the indication proposed in ASTM D-2940 Standard Specification for Graded Aggregate Material (2015), which is 0.5%, for bases and sub-bases of highways and airports, but in all the cases, they are less than 1%, a limit value indicated in less exigent countries for hydraulic and bituminous concretes (WSDOT, 2015). Only one curve displayed a delayed peak at about 7 hours; in that case, an undesired anomaly during swelling record appeared, as it was demonstrated by a flat branch lasting for the further duration of the test.

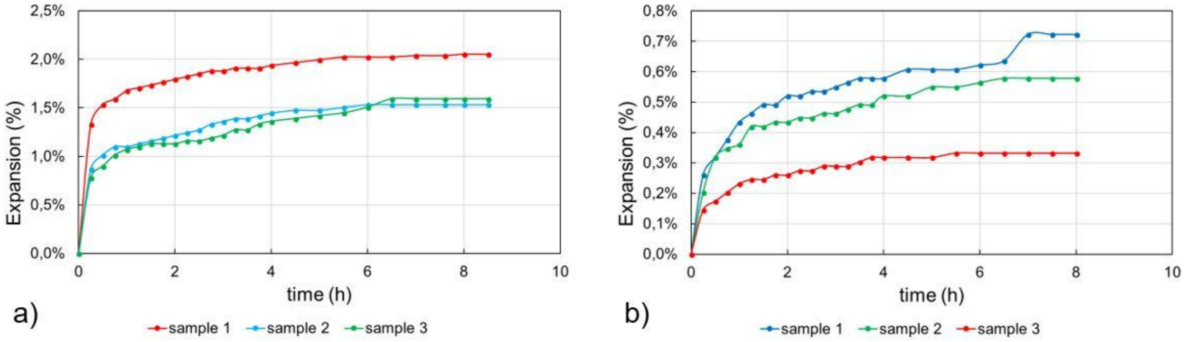

Figure 10. Expansion test results carried out on: a) fresh slag samples; b) weathered slag samples. Curves are cut after 8 hours form the initial time as no further expansion occurred.

Further two tests were carried out on fresh slag. Slag was dried, sieved and then placed into a mold as a sample of non-well graded pieces, made mainly of coarse particles (gap-graded sample). Subsequently, this sample was compacted in the mold, and subject to the steam flow. After testing, the resultant slag pieces were crushed and combined to fit, as much as possible, Fuller grading curve with lower maximum size of aggregate than the former test (re-crushed sample). In such way, new available specific surface was provided for further hydration, which occurred re-testing the sample. Results of this new test are reported in Figure 11: it is possible to see how slag expanded again after further crushing. Undoubtedly, the mentioned delayed hydration and carbonation of free CaO and free periclase can be activated. In ordinary condition, i.e. when slag is placed in construction works and particularly in concrete with low permeability, such long-term swelling might be neither not activated, because of the non-accessibility of moisture to secondary lime.

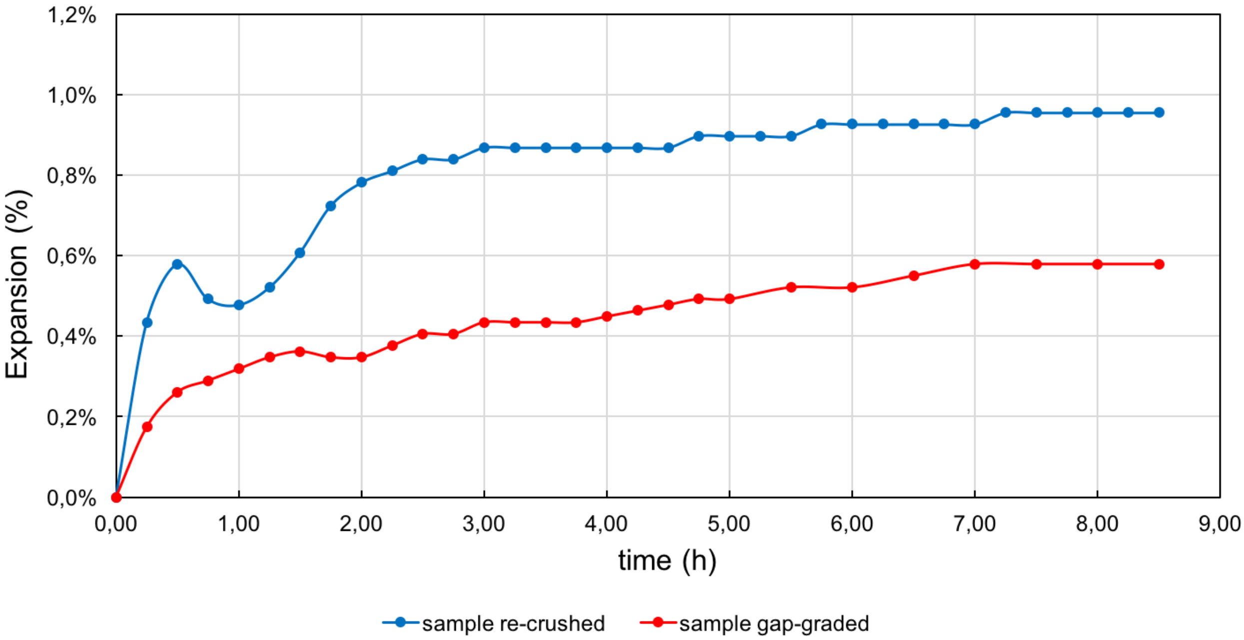

Figure 11. Expansion test results carried out on fresh gap-graded sample, and re-crushed slag.

The obtained results demonstrate the reliability and affordability of the use of electric arc oxidizing slag in construction and building after a simple stabilization treatment, by weathering at outdoor exposition. After this treatment, the potential swelling of this slag is about 0.5%, a tolerable value in most of the current standards, and considered also by the authors of this work as a reliable limit for applications in cement-based matrix. Additionally, a less restrictive limit of 1.0% can be also considered for applications in bituminous-bounded matrixes, according to authors experience. It is worth noting how such treatment is essential in reducing potential swelling, and particularly it should be performed after the operations of crushing and sieving of the aggregates, in order to do not provide further available specific surface for potential hydration of free CaO when processed. However, many variables may be present during slag production, depending on the operating conditions inside the furnace, slag cooling, etc., which influence slag physical and chemical properties. Instead, a different behavior is expected when managing ladle furnace slag, which is also a by-product in EAF steel plants. Indeed, such slag might contain MgO quantities as higher as 10%; in this case, long-term swelling represents the main obstacle for its use in civil engineering applications (Yildirim and Prezzi, 2017). Volumetric strains of 0.98% and 0.83% at about 16 months of ageing have been recorded, without the evidence of developing any steady state or expansion reduction.

The presence of an outstanding amount of calcite in the external surface of slag particles after weathering is a positive factor, which allows also an increase of its performance when used in hydraulic and bituminous mixes. Indeed, surface texture allows the development of the often observed excellent adhesion and compatibility of calcite with the classical binders present in civil engineering materials, i.e., bituminous products and cementitious pastes (Mehta and Monteiro, 2013).

5. Conclusions

This work has analyzed the problem of EAFS swelling potential with a detailed approach, based both on a chemical and physical characterization of slag particles, and also on expansion tests based on steam diffusion, carried out on samples of both fresh and weathered slag.

Based on the experimental evidences obtained in this work, the following conclusions can be drawn:

- hydroxylation of free CaO and subsequent carbonation in presence of moisture is considered as the most relevant reaction responsible for EAFS expansion;
- if hydroxylation of free CaO is controlled, i.e., if operators allow its development after a specific weathering and curing treatment, such phenomenon can even improve slag properties, due to the formation of a layer of calcite onto the slag surface;
- slag surface enrichment in calcite promotes a better bond of slag particles with the matrixes where they are employed, e.g. with cement pastes and bitumen;
- open porosity of slag can be filled by hydration products, resulting in a less porous aggregate, thus improving again mechanical performance;
- slag re-crushing, without any subsequent dimensional stabilization treatment (e.g., water spraying) is not recommended, because it might activate again slag swelling due to the new available slag surface.

Acknowledgments

This work is supported by the Spanish Ministry MINECO and FEDER Funds for financial support through Project BlueCons: BIA2014-55576-C2-2-R. The authors would to express their gratitude to the Vice-Rectorate of Investigation of the University of the Basque Country for grant PIF 2013, the grant for mobility of researchers 2015 and, likewise, to the Basque Government for financial support to Research Group IT781-13. The authors would also to acknowledge Acciaierie Venete SpA and ZeroCento Srl for supplying raw materials.

References

Adegoloye, G., Beaucour, A.-L., Ortola, S., Noumowe, A. 2016. Mineralogical composition of EAF slag and stabilised AOD slag aggregates and dimensional stability of slag aggregate concretes. Constr. Build. Mater. 115, 171-178. https://doi.org/10.1016/j.conbuildmat.2016.04.036.

Akinmusuru, J.O., 1991. Potential beneficial uses of steel slag wastes for civil engineering purposes. Resour. Conserv. Recycl. 5 (1), 73-80. https://doi.org/10.1016/0921-3449(91)90041-L.

Al-Negheimish, A.I., Al-Sugair, F.H., Al-Zaid, R.Z. 1997. Utilization of local steel making slag in concrete. Journal of King Saud University. 9, 39-55.

Ameri, M., Hesami, S., Goli, H. 2013. Laboratory evaluation of warm mix asphalt mixtures containing electric arc furnace (EAF) steel slag. Constr. Build. Mater. 49, 611-617. https://doi.org/10.1016/j.conbuildmat.2013.08.034.

Anastasiou, E., Georgiadis Filikas, K., Stefanidou, M. 2014. Utilization of fine recycled aggregates in concrete with fly ash and steel slag. Constr. Build. Mater. 50, 154-161. https://doi.org/10.1016/j.conbuildmat.2013.09.037.

Arribas, I., San-José, J.T., Vegas, I.J., Hurtado, J.A., Chica, J.A. 2010. Application of steel slag concrete in the foundation slab and basement wall of the TECNALIA Kubik Building. In: Ferrous slag – resource development for an environmentally sustainable world, Proceedings of the 6th European slag conference, EUROSLAG Publication No. 5, Madrid, Spain, pp.251–64.

Arribas, I., Vegas, I., San-José, J.T., Manso, J.M. 2014. Durability studies on steelmaking slag concretes. Mater. Des. 63, 168-176. https://doi.org/10.1016/j.matdes.2014.06.002.

Arribas, I., Santamaría, A., Ruiz, E., Ortega-López, V., Manso, J.M. 2015. Electric arc furnace slag and its use in hydraulic concrete. Constr. Build. Mater. 90, 68-79. https://doi.org/10.1016/j.conbuildmat.2015.05.003.

ASTM D2940/D2940M 2015. Standard Specification for Graded Aggregate Material For Bases or Subbases for Highways or Airport. ASTM International, 100 Barr Harbour Dr. P.O. box C-700 West Conshohocken, Pennsylvania, United States.

Autelitano, F., Giuliani, F. 2015. Swelling Behavior of Electric Arc Furnace Aggregates for Unbound Granular Mixtures in Road Construction. International Journal of Pavement Research and Technology. 8 (2), 103-111. http://dx.doi.org/10.6135/ijprt.org.tw/2015.8(2).103.

Bosela, P., Delatte, N., Obratil, R., Patel, A. 2009. Fresh and hardened properties of paving concrete with steel slag aggregate. Propiedades para firmes de hormigón fabricado con áridpos siderúrgicos. Revista Técnica de la asociación española de carreteras. 166, 55-66.

Bignozzi, M.C., Sandrolini, F., Andreola, F., Barbieri, L., Lancellotti, I. 2010. Recycling electric arc furnace slag as unconventional component for building materials. In: Zachar, J., Claisse, P., Naik, T.R., Ganjian, E. (Eds.), Proceeding of 2nd International Conference on Sustainable Construction Materials and Technologies, Milwaukee, pp. 557-567.

Brand, A.S., Roesler, J.R., 2015. Steel furnace slag aggregate expansion and hardened concrete. Cem. Concr. Comp. 60, 1-9. http://dx.doi.org/10.1016/j.cemconcomp.2015.04.006

Colorado, H.A., Garcia, E., Buchely, M.F. 2016. White Ordinary Portland Cement blended with superfine steel dust with high zinc oxide contents. Constr. Build. Mater. 112, 816-824. https://doi.org/10.1016/j.conbuildmat.2016.02.201.

Coppola, L., Lorenzi, S., Buoso, A. 2010. Electric arc furnace granulated slag as a partial replacement of natural aggregates for concrete production. Web proceeding of 2nd International Conference on Sustainable

Construction Materials and Technologies. http://www.claisse.info/2010%20papers/web.htm (accessed 02 February 2018).

DePree, P.J., Ferry, C.T. 2008. Mitigation of Expansive Electric Arc Furnace Slag in Brownfield Redevelopment. In: Proceedings of GeoCongress 2008: Geosustainability and Geohazard Mitigation, pp. 271-278.

EN 12620:2002-A1:2008 (2002) Aggregates for concrete. Comité Européen de Normalisation, Brussels, Belgium.

EN 1744-1:2009+A1:2012 (2012) Tests for chemical properties of aggregates - Part 1: Chemical analysis. Comité Européen de Normalisation, Brussels, Belgium,

Faleschini, F., De Marzi, P., Pellegrino, C. 2014. Recycled concrete containing EAF slag: Environmental assessment through LCA. Eur. J. Environ. Civ. Eng. 18 (9) 1009-1024. https://doi.org/10.1080/19648189.2014.922505.

Faleschini, F., Alejandro Fernández-Ruíz, M., Zanini, M.A., Brunelli, K., Pellegrino, C., Hernández-Montes, E. 2015. High performance concrete with electric arc furnace slag as aggregate: mechanical and durability properties. Constr. Build. Mater. 101, 113-121. https://doi.org/10.1016/j.conbuildmat.2015.10.022.

Faleschini, F., Brunelli, K., Zanini, M.A., Dabalà, M., Pellegrino, C. 2016. Electric Arc Furnace Slag as Coarse Recycled Aggregate for Concrete Production. Journal of Sustainable Metallurgy. 2 (1), 44-50. doi: 10.1007/s40831-015-0029-1.

Faleschini, F., Hofer, L., Zanini, M.A., Dalla Benetta, M., Pellegrino, C. 2017. Experimental behavior of beam-column joints made with EAF concrete under cyclic loading. Eng. Struct. 139, 81-95. https://doi.org/10.1016/j.engstruct.2017.02.038.

Frías, M., San-José, J., Vegas, I. 2010. Steel slag aggregate in concrete: the effect of ageing on potentially expansive compounds. Materiales de Construcción 60 (297), 33-46. 10.3989/mc.2019.45007.

Fronek, B.A. 2012. Feasibility of Expanding the use of Steel Slag as a Concrete Pavement Aggregate. Bachelor of Civil Engineering. Cleveland State University.

Fronek, B., Bosela, P., Delatte, N. 2012. Steel slag aggregate used in Portland cement concrete: U.S. and international perspectives. Transp. Res. Rec. 2267, 37-42. https://doi.org/10.3141/2267-04.

Fuente-Alonso, J.A., Ortega-López, V., Skaf, M., Aragón, A., San-José, J.T. 2017. Performance of fiber-reinforced EAF slag concrete for use in pavements. Constr. Build. Mater. 149, 629-638

García Mochales, J.L. 2016. Utilización de áridos siderúrgicos en obras por la autoridad portuaria de Bilbao. Jornada sobre RECICLAJE de RESIDUOS como MATERIALES ALTERNATIVOS de CONSTRUCCION, 22 April 2015, Universidad de Zaragoza, Spain.

Geiseler, J., 1996. Use of steelworks slag in Europe. Waste Manage. 16, 59-63. https://doi.org/10.1016/S0956-053X(96)00070-0.

Geiseler, J., Schlösser, R. 1998. Investigation concerning the structure and properties of steel slags. In: Proceedings of the 3rd International Conference on molten slags and fluxes. Glasgow, Scotland, pp. 40-42.

Herrero, T., Vegas, I. J., Santamaría, A., San-José, J. T., Skaf, M. 2016. Effect of high-alumina ladle furnace slag as cement substitution in masonry mortars. Constr. Build. Mater. 123, 404-413. https://doi.org/10.1016/j.conbuildmat.2016.07.014.

IHOBE.1999. Libro blanco para la minimización de residuos y emisiones: escorias de acería. IHOBE (Eds.). pp.1-131.

Kavussi, A., Qazizadeh, M.J. 2014. Fatigue characterization of asphalt mixes containing electric arc furnace (EAF) steel slag subjected to long term aging. Constr. Build. Mater. 72, 158-66. https://doi.org/10.1016/j.conbuildmat.2014.08.052.

Kim, S-W., Kim, Y-S., Lee J-M., Kim, K-H. 2013.Structural performance of spirally confined concrete with EAF oxidising slag aggregate. Eur. J. Civ. Environ. Eng. 17 (8), 654-674. https://doi.org/10.1080/19648189.2013.810178.

Koros, P.J., 2003. Dusts, scale, slags, sludges... Not wastes, but sources of profits. Metallurgical and Materials Transactions B. 34 (6), 769-779. https://doi.org/10.1007/s11663-003-0083-0.

Manso, J.M., Polanco, J.A., Losañez, M., González, J.J. 2006. Durability of concrete made with EAF slag as aggregate. Cem. Concr. Compos. 28, 528-34. https://doi.org/10.1016/j.cemconcomp.2006.02.008.

Manso, J.M., Ortega-López, V., Polanco, J.A., Setién, J. 2013. The use of ladle furnace slag in soil stabilization. Constr. Build. Mater. 40, 126-134. https://doi.org/10.1016/j.conbuildmat.2012.09.079.

Mehta, P.K., Monteiro, P.J.M. 2013. Concrete: Microstructure, Properties, and Materials. McGraw Hills.

Monosi, S., Ruello, M.L., Sani, D. 2016. Electric arc furnace slag as natural aggregate replacement in concrete production. Cem. Concr. Compos. 66, 66-72. https://doi.org/10.1016/j.cemconcomp.2015.10.004.

Morino, K., Iwatsuki, E. 1999. Durability of concrete using electric arc furnace oxidizing slag aggregates. In: Swamy (eds.). Infrastructure regeneration and rehabilitation improving the quality of life through better construction International conference. Sheffield, pp. 213-222.

Motz, H., Geiseler, J., 2001. Products of steel slags an opportunity to save natural resources. Waste Manage. 21 (3), 285-293. https://doi.org/10.1016/S0956-053X(00)00102-1.

Oluwasola, E.A., Hainin, M.R., Aziz, M.M.A. 2015. Evaluation of rutting potential and skid resistance of hot mix asphalt incorporating electric arc furnace steel slag and copper mine tailings. Indian J. Eng. Mater. Sci. 22, 550-558.

Oluwasola, E.A., Hainin, M.R., Aziz, M.M.A. 2016. Comparative evaluation of dense-graded and gap-graded asphalt mix incorporating electric arc furnace steel slag and copper mine tailings. J. Clean. Prod. 122, 315-325. https://doi.org/10.1016/j.jclepro.2016.02.051.

Ortega-López, V., Manso, J.M., Cuesta, I.I., González, J.J. 2014 The long-term accelerated expansion of various ladle-furnace basic slags and their soil-stabilization applications. Constr. Build. Mater. 68, 455-464. https://doi.org/10.1016/j.conbuildmat.2014.07.023

Ortega-Lopez, V., Fuente-Alonso, J.A., Santamaría, A., San-José, J.T., Manso, J.M. 2018. Durability studies on fiber-reinforces EAF slag concrete for pavements. Constr. Build. Mater. 163, 471-481.

Papayianni, I., Anastasiou, E. 2010. Production of high-strength concrete using high volume of industrial by-products. Constr. Build. Mater. 24, 1412-1417. https://doi.org/10.1016/j.conbuildmat.2010.01.016.

Pasetto, M., Baldo, N., 2006. Electric arc furnace steel slags in "high performance" asphalt mixes: a laboratory characterization. in: Key lecture, TMS Fall Extraction and Processing Division: Sohn’s International Symposium 5, San Diego, USA, 2006, pp. 443–450.

Pasetto, M., Baldo, N. 2011. Mix design and performance analysis of asphalt concretes with electric arc furnace slag. Constr. Build. Mater. 25, 3458-3468. https://doi.org/10.1016/j.conbuildmat.2011.03.037.

Pasetto, M., Baldo, N. 2012. Fatigue characterization of asphalt rubber mixtures with steel slags. RILEM Bookseries 4. Springer, Netherlands, pp. 729-37.

Pasetto, M., Baldo, N. 2014. Foamed bitumen bound mixtures made with marginal aggregates: an experimental study. In: Losa & Papagiannakis (Eds.). Sustainability, Eco-efficiency, and Conservation in Transportation Infrastructure Asset Management, CRC Press, Taylor & Francis Group, London. pp. 3-13.

Pasetto, M., Baldo, N. 2016. Recycling of waste aggregate in cement bound mixtures for road pavement bases and sub-bases. Constr. Build. Mater. 108, 112-118. https://doi.org/10.1016/j.conbuildmat.2016.01.023.

Pasetto, M., Giacomello, G., Pasquini, E., Canestrari, F. 2016. Effect of warm mix chemical additives on the binder-aggregate bond strength and high-service temperature performance of asphalt mixes containing electric arc furnace steel slag. RILEM Bookseries 11. Springer, Netherlands, pp. 485-96.

Pasetto, M., Baliello, A., Giacomello, G., Pasquini, E. 2017. Sustainable solutions for road pavements: a multi-scale characterization of warm mix asphalts containing steel slags. J. Clean. Prod. 166 (6), 835-843.

Pellegrino, C., Cavagnis, P., Faleschini, F., Brunelli, K. 2013. Properties of concretes with Black/Oxidizing Electric Arc Furnace slag aggregate. Cem. Concr. Compos. 37, 232-240. https://doi.org/10.1016/j.cemconcomp.2012.09.001.

Pellegrino, C., Faleschini, F. 2013. Experimental behavior of reinforced concrete beams with electric arc furnace slag as recycled aggregate. ACI Mater. J. 110, 197-206.

Pellegrino C., Gaddo V. 2009. Mechanical and durability characteristics of concrete containing EAF slag as aggregate. Cem. Concr. Compos. 31(9), 663-671.

Pellegrino C., Faleschini F. 2016. Experimental Database of EAF Slag Use in Concrete. Sustainability Improvements in the Concrete Industry, Green Energy and Technology, doi: 10.1007/978-3-319-28540-5_6.

Santamaría, A., Rojí, E., Skaf, M., Marcos, I., González, J.J. 2016. The use of steelmaking slags and fly ash in structural mortars. Constr. Build. Mater. 106, 364-373. https://doi.org/10.1016/j.conbuildmat.2015.12.121.

Santamaría, A., Faleschini, F., Vegas, I., San-José, J.-T., Pellegrino C., González, J.J. 2017. A comparison between European Electric Arc Furnace slags. Proceedings of the Euroslag 2017, Metz, France.

Sekaran, A., Palaniswamy, M., Balaraju, S. 2015. A Study on Suitability of EAF Oxidizing Slag in Concrete: An Eco-Friendly and Sustainable Replacement for Natural Coarse Aggregate. The Scientific World Journal 2015, 1-8. http://dx.doi.org/10.1155/2015/972567.

Shelburne, W., DeGroot, D.J. 1998. The use of waste and recycled materials in highway construction. Civ. Eng. Pract. 13, 5-16.

Skaf, M., Ortega-López, V., Fuente-Alonso, J.A., Santamaría, A., Manso, J.M. 2016. Ladle furnace slag in asphalt mixes. Constr. Build. Mater. 122, 488-495. https://doi.org/10.1016/j.conbuildmat.2016.06.085.

Skaf, M., Manso, J.M., Aragón, Á., Fuente-Alonso, J.A., Ortega-López, V. 2017. EAF slag in asphalt mixes: A brief review of its possible re-use. Resour. Conserv. Recycl. 120, 176-185. https://doi.org/10.1016/j.resconrec.2016.12.009.

Tomellini, R. 1999 Summary report on RTD in iron and steel slags: development and perspectives. Technical Steel Research, Report Prepared for the European Commission EUR 19066, Brussels, Belgium.

Wachsmuth, F., Geiseler, J., Fix, W., Koch, K. Schwerdtfeger, K. 1981. Contribution to the structure of BOF-slags and its influence on their volume stability. Canadian Metallurgical Quarterly 20, 279-284.

Waligora, J., Bulteel, D., Degrugilliers, P., Damidot, D., Potdevin, J.L., Measson, M. 2010. Chemical and mineralogical characterizations of LD converter steel slags: A multi-analytical techniques approach. Mater. Charact. 61, 39-48. https://doi.org/10.1016/j.matchar.2009.10.004.

Wang, G. 2010. Determination of the expansion force of coarse steel slag aggregate. Constr. Build. Mater. 24, 1961-1966. https://doi.org/10.1016/j.conbuildmat.2010.04.004.

Wang, G., Wang, Y., Gao, Z. 2010. Use of steel slag as a granular material: Volume expansion prediction and usability criteria. J. Hazard. Mater. 184, 555-560. https://doi.org/10.1016/j.jhazmat.2010.08.071.

Wang, W.C., Liu, C.C., Lee, C. 2015. Effect of a small addition of highly expansive slag on volume stability of cement matrix material. Journal of Asian Concrete Federation. 1 (1), 57-63. https://doi.org/10.18702/acf.2015.09.1.57.

Worldsteel association, 2015. Steel Statistical Yearbook, First Ed. Brussels.

WSDOT Strategies Regarding Use of Steel Slag Aggregate in Pavements (2015) A Report to the State Legislature In Response to 2ESHB 1299. Washington State DOT Construction Division Pavements Office

Yildirim, I.Z., Prezzi, M. 2009. Use of steel slag in subgrade applications. Publication FHWA/IN/JTRP-2009/32. Joint Transportation Research Program, Indiana Department of Transportation and Purdue University, West Lafayette, Indiana. https://doi.org/10.5703/1288284314275.

Yildirim, I.Z., Prezzi, M. 2011. Chemical, mineralogical, and morphological properties of steel slag. Advances in Civil Engineering. 2011. pp 1-13. http://dx.doi.org/10.1155/2011/463638.

Yildirim, I.Z., Prezzi, M. 2017. Experimental evaluation of EAF ladle steel slag as a geo-fill material: Mineralogical, physical & mechanical properties. Constr. Build. Mater. 154, 23-33. http://dx.doi.org/10.1016/j.conbuildmat.2017.07.149